Journal of Materials Chemistry A

PAPER

View Article Online
View Journal | View Issue

Cite this: J. Mater. Chem. A, 2015, 3, 11511

Design of an enzymatic biofuel cell with large power output†

Yun Chen,‡[a] Panpan Gai,‡[a] Jianrong Zhang*[ab] and Jun-Jie Zhu*[a]

Received 23rd February 2015
Accepted 20th April 2015

DOI: 10.1039/c5ta01432h

www.rsc.org/MaterialsA

Enzymatic biofuel cells (EBFCs) utilize redox enzymes as the catalysts to produce energy from green and renewable fuels, and are considered as promising, environmentally friendly power sources. However, EBFCs are limited by the relatively slow rate of electron transfer between enzymes and electrodes, which is a major barrier to improving EBFC power output. In this study, enzymes were bound to the hydrophilic, carboxyl group functionalized graphene–gold nanoparticle hybrid, and the hybrid as electrode material was able to increase the rate of electron transfer in the EBFC. The open-circuit voltage (E_{cell}^{ocv}) of this designed EBFC reached 1.16 ± 0.02 V, and the maximal power density (P_{max}) was as high as 1.96 ± 0.13 mW cm^{-2}. Two as-prepared EBFC units arranged in series were able to light up red and yellow light-emitting diodes (LEDs). Also, using these EBFCs, the E_{cell}^{ocv} and P_{max} retained 80% and 66% of their optimal values over 70 days, respectively. This fabricated EBFC is expected to find applications in the bioenergy fields.

1. Introduction

In order to overcome the ever-worsening crises due to traditional non-renewable energy consumption, researchers have tried to find efficient methods for converting chemical energy into electrical energy.[1] Biofuel cells (BFCs) that use enzymes (enzymatic biofuel cells, EBFCs) or microorganisms as catalysts are able to oxidize targeted biofuels and reduce oxidizers at specific electrodes to harvest energy.[1–4] Compared to traditional fuel cells, BFCs offer special advantages. First, unlike the noble metal catalysts, which are expensive and have limited storage, biological catalysts have plentiful and reproducible sources. Second, in BFCs, the renewable biofuels from plants and animals are used as fuels at the anode, while O_2 usually serves as the oxidizer at the cathode. Because the products of the reaction in BFCs are non-toxic,[5] BFCs are biocompatible and can be miniaturized for use as an implantable power supply for medical devices.[3,6–8] Finally, most of the BFCs can generate electricity under mild conditions. As a result, BFCs are predicted to be one of the next-generation green sustainable energy devices.

Although BFCs represent a new power source, it is still difficult to apply them commercially. In contrast to the traditional fuel cells, the applicability of BFCs is limited by several factors, including low open-circuit voltage (E_{cell}^{ocv}), insufficient power output, and long-term instability.[1,2] Generally, in the case of EBFCs, glucose oxidase (GOx) is used for catalyzing the oxidation of glucose at the anode, and laccase is applied to the reduction of O_2 at the cathode. Note, however, that the formation of electrical contacts between the redox enzymes and the electrodes is of fundamental significance for the development of EBFCs,[9] but because the active centres of most redox enzymes are deeply buried within the protein interior, it is difficult to achieve direct electron transfer (DET) between the enzymes and the electrodes.[1–3] The poor electron transfer results in the low power densities of EBFCs. To date, the greatest E_{cell}^{ocv} for a single EBFC unit has been reported to be 0.95 V.[10,11] The maximal power density (P_{max}) reached has been reported to be 1.45 ± 0.24 mW cm^{-2},[12] and active lifetimes typically between 8 hours and 30 days.[1,10]

Nanoparticles with high electrochemical stability and good conductivity can be selected to form ideal conducting channels to promote efficient DET between enzymes and electrodes.[4] Recently, we fabricated a hybrid of hydrophilic carboxyl group functionalized graphene–gold nanoparticles (AuNPs) for electrochemical biosensing of glucose,[13] and demonstrated that the hybrid could provide a suitable microenvironment for GOx to retain its biological activity. The DET between GOx and the hybrid electrode could be realized without an electron mediator.

Herein, the graphene–AuNP hybrid electrode was used for designing an EBFC, as shown in Scheme 1. The morphology of the graphene–AuNP hybrid is shown in Fig. S1 in the ESI.† In the bioanode compartment, GOx bound to the graphene–AuNP

[a]State Key Laboratory of Analytical Chemistry for Life Science, School of Chemistry and Chemical Engineering, Nanjing University, Nanjing, 210093, P. R. China. E-mail: jrzhang@nju.edu.cn; jjzhu@nju.edu.cn; Fax: +86 25 83594976; Tel: +86 25 83686130
[b]School of Chemistry and Life Science, Nanjing University Jinling College, Nanjing 210089, P. R. China

† Electronic supplementary information (ESI) available. See DOI: 10.1039/c5ta01432h

‡ These authors contributed equally to this work.

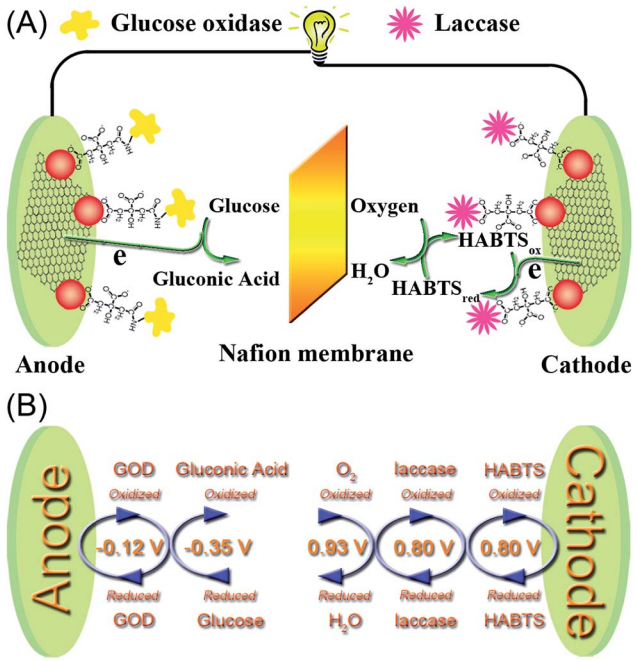

Scheme 1 (A) Principle of operation of the EBFC based on the graphene–AuNP hybrid anode and cathode, and (B) the formal redox potentials (*vs.* SHE, pH = 5.0) schematic for the EBFC.

hybrid,[13] and glucose was oxidized to gluconolactone without a redox mediator under anaerobic conditions; gluconolactone was further oxidized to gluconic acid by the graphene–AuNP hybrid. The electrons produced in the bioanode compartment flowed through an external circuit load to the biocathode compartment, where O_2 was reduced to H_2O. The biocathode was composed of laccase bound to the graphene–AuNP hybrid as a biocatalyzer, and 2,2′-azinobis(3-ethylbenzothiazoline-6-sulfonic acid) diammonium salt (ABTS) as a redox mediator (saturated with O_2). Because laccase is often inactive at neutral pH, and usually requires an environment of pH 5.0,[5,14] the acetic acid buffer solution was selected as the electrolyte. The two compartments were separated with a nafion membrane. In the EBFC, the E_{cell}^{ocv} and the P_{max} reached 1.16 ± 0.02 V and 1.96 ± 0.13 mW cm^{-2}, respectively, and E_{cell}^{ocv} and P_{max} retained 80% and 66% of their optimal values after 70 days, respectively. Red and yellow light-emitting diodes (LEDs) were successfully lit by two as-fabricated EBFC units in series.

2. Experimental

2.1 Chemicals

The hydrophilic, carboxyl group-functionalized graphene–AuNP hybrid, which was suitable for the binding of enzymes stably by the condensation reaction with the amino group, was fabricated as reported in our previous work.[13] GOx from *Aspergillus niger* (EC 1.1.3.4, 294 units per mg) was purchased from Sanland. Laccase from *Trametes versicolor* (EC 1.10.3.2, >20 units per mg) and ABTS were obtained from Sigma-Aldrich. Both of the enzymes were used as received without further purification. Glucose was obtained from Sinopharm, and the glucose stock solution (1 M) was prepared at least 24 h before use. 0.2 M acetic acid buffer solution (pH 5.0) was made from acetic acid and sodium acetate anhydrous. Aqueous solutions were prepared with ultrapure water from an Elix 5 Pure Water System (>18 MΩ cm).

2.2 Instrumentation

The morphology of the graphene–AuNP hybrid was characterized by field emission scanning electron microscopy (FESEM, HITACHI S4800). Electrochemical measurements were performed using a workstation (CHI 660B). Cyclic voltammetric measurements were performed with a traditional three-electrode system including a Pt wire electrode as the counter electrode, a saturated calomel electrode (SCE) as the reference electrode, and the modified Au substrate as the working electrode. The open-circuit potentials of the electrodes were tested with a two-electrode configuration (SCE as the reference electrode).

2.3 Preparation of bioanode and biocathode

The Au substrates (1 cm × 0.5 cm) were provided by the 55th Institute of the China Electronic Group (Nanjing, China). The Au substrates were prepared by sputtering 200 nm Au onto quartz wafers with a few nanometers of a Cr adhesion layer in a vacuum.[15] Before use, the Au substrates were carefully scraped to a mirror finish by using pledget, then rinsed and sonicated with ethanol and ultrapure water, respectively, and dried under nitrogen flow.

The bioanode of the EBFC was fabricated as reported previously.[13] Under conditions determined in this work to be optimum, 240 μg cm^{-2} graphene–AuNP hybrid was dropped onto the Au substrate, and then the electrode was dried in an oven desiccator and stored at 37 °C. Then, the graphene–AuNP hybrid electrode was immersed in a solution containing 1 mg mL^{-1} 1-ethyl-3-(3-dimethyl-aminopropyl) carbodiimide hydrochloride (EDC) and *N*-hydroxysuccinimide (NHS) for 3 h. After rinsing with ultrapure water to get rid of the excess EDC and NHS, the activated electrodes were immersed in 1 mL of GOx solution (10 mg mL^{-1}, dissolved in 0.05 M pH 9.0 Tris–HCl solution) at 4 °C for 24 h. The biocathode of the EBFC was prepared as follows: after the fabrication of the graphene–AuNP hybrid electrode, 50 μL of the laccase solution (60 mg mL^{-1}, dissolved in 0.05 M pH 7.0 PBS solution) was dropped onto the graphene–AuNP hybrid electrode and stored at 4 °C; before the assembly of the EBFC, both the prepared graphene–AuNP–GOx hybrid electrode and the graphene–AuNP–laccase hybrid electrode were purged with ultrapure water to wipe off unbound enzymes, and the electrodes were stored at 4 °C when they were not in use.

2.4 Biofuel cell design

The perfluorosulfonic acid/PTFE copolymer membrane (DuPont™ Nafion® PFSA NRE-211), with a thickness 25.4 μm, was used to separate the anodic and cathodic compartments. The anolyte was 0.2 M acetic acid buffer solution (pH 5.0) containing 50 mM of glucose saturated with nitrogen. An

oxygen-saturated 0.2 M acetic acid buffer solution (pH 5.0) containing 0.5 mM of ABTS acted as the catholyte. The EBFC was operated at room temperature (25 °C). After a stable E_{cell}^{ocv} was observed, a variable external load ranging from 100 Ω to 100 kΩ was connected in series between the anode and cathode. Then the power outputs were obtained with a precision digital multimeter.

3. Results and discussion

3.1 The characteristics of the bioanode

In the bioanode, glucose oxidase first catalyzes the oxidation of β-D-glucose to D-glucono-1,5-lactone as follows: glucose → gluconolactone + $2H^+$ + 2e ($\varphi' = -0.24$ V *vs.* SHE at pH 5.0). However, D-glucono-1,5-lactone can be hydrolyzed to gluconic acid further, but this hydrolysis is not fast enough. According to Claus,[16] gold nanoparticle–carbon materials constitute the preferred catalyst for the oxidation of the –OH and C=O functional groups. Therefore, the gold nanoparticle–graphene hybrid in the bioanode can thoroughly oxidize glucose to gluconic acid, and the reaction at the bioanode should be

$$\text{glucose} \xrightarrow{\text{GOx,graphene–AuNP}} \text{gluconic acid} + 2H^+ + 2e \qquad E_a^{o'} = -0.35\ \text{V}(vs.\ \text{SHE}) \tag{1}$$

where $E_a^{o'}$ is the formal potential at pH 5.0, and the potential of −0.35 V (*vs.* SHE) is calculated using the Nernst equation according to the formal potential of the gluconic acid/glucose couple ($E_a^{o'} = -0.45$ V *vs.* SHE) at pH 7.0.[17] Under the open-circuit potential (OCP) condition, when SCE was used as the reference electrode ($E_{ref} = 0.24$ V), E_a^{ocp} was calculated to be −0.59 V. The measurement of the E_a^{ocp} was performed in a 0.2 M acetic acid buffer solution (pH 5.0) saturated with N_2. E_a^{ocp} was recorded immediately after the circuit was closed, and the onset of E_a^{ocp} was −0.36 V (or −0.12 V *vs.* SHE) (Fig. 1A), which was equal to the formal potential of GOx ($E_{GOx}^{o'}$) as shown in Scheme 1B. As seen in curve b of Fig. 1A, E_a^{ocp} rapidly reached and then stayed at −0.58 ± 0.01 V ($n = 3$) (or −0.34 V *vs.* SHE), approaching the speculated value, when there was 50 mM glucose in the testing solution. The speculated value was the formal potential of gluconic acid/glucose at pH 5.0, with SCE as reference electrode (E_a^{ocp}). As seen in curve a of Fig. 1A, however, E_a^{ocp} only reached 0.062 ± 0.012 V ($n = 3$) when there was no glucose in the testing solution. The E_a^{ocp} result demonstrated that the OCP of the bioanode was eventually determined by the thermodynamic potential of the fuel, *i.e.*, the gluconic acid/glucose couple.[18,19]

The current density (i) in the bioanode influences the power output of the EBFC, which can be expressed as follows:

$$i = nFk^0[\Gamma_O(0, t)e^{-\alpha f(E-E^{o'})} - \Gamma_R(0, t)e^{(1-\alpha)f(E-E^{o'})} \tag{2}$$

where the meanings of the symbols are the same as described previously.[20] According to eqn (2), i relies on the electron-transfer rate constant (k^0), which is affected by the electrode materials. In our previous measurement of the graphene–AuNP–GOx hybrid with a glass carbon substrate electrode, k^0, the rate of the direct electron transfer of GOx, was evaluated as 7.74 ± 0.16 s^{-1}.[13] For comparison, Au was selected as the substrate electrode in the fabrication of the bioanode. Cyclic voltammograms (CVs) of the Au electrode modified with the graphene–AuNP hybrid (curve a) and that modified with the graphene–AuNP–GOx hybrid (curve b) are shown in Fig. 1B, and Fig. S2 in the ESI† also shows CVs of Au electrodes modified with AuNPs, graphene, AuNPs–GOx, and graphene–GOx, respectively. In contrast to curve a in Fig. 1B, curve b in Fig. 1B shows a couple of well-defined redox peaks, at −0.38 and −0.35 V, which can be ascribed to the characteristic peaks of GOx (see also Fig. S3 in the ESI†).[21] The peak-to-peak separation and the formal potential for GOx were obtained accordingly, and were determined to be 29 mV and −0.36 V (or −0.12 V *vs.* SHE), respectively, and k^0 was calculated to be 12.50 ± 0.27 s^{-1}. Compared to curve b in Fig. 1B, curve c showed that the oxidative peak increased while the reductive peak decreased when 1 mM glucose was added into the testing solution, which demonstrated that graphene–AuNP–GOx could bioelectrocatalyze the oxidation of glucose directly in an E_rC_i-type catalytic reaction.[20] However, CVs for the graphene electrode and for the AuNP electrode were nearly unaffected by the presence of glucose in the testing solution. The results support the notion that the electron transfer from glucose to the electrode *via* GOx was extremely fast, and that Au was also the more suitable substrate material for the bioanode modified with the graphene–AuNP–GOx hybrid.

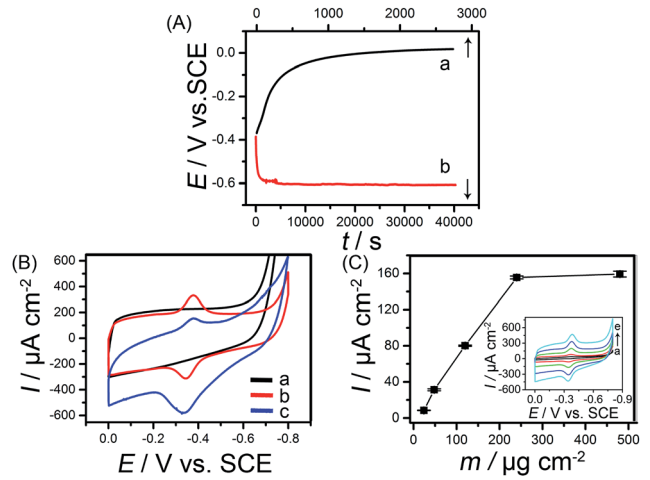

Fig. 1 (A) OCP of the graphene–AuNP–GOx hybrid electrode in a pH 5.0 electrolyte solution (a) without glucose and (b) with 50 mM glucose. (B) CVs of (a) graphene–AuNP hybrid electrode, (b) graphene–AuNP–GOx hybrid electrode only in pH 5.0 buffer solution and (c) graphene–AuNP–GOx hybrid electrode in pH 5.0 electrolyte solution containing 1 mM glucose. (C) The relationship between the reduction peak currents of the bound GOx and the amount of the graphene–AuNP hybrid only in pH 5.0 buffer solution. Each point on the graph was calculated by taking the average of three independent measurements. Inset: CVs of graphene–AuNP–GOx hybrid electrodes with various area densities of the hybrid: (a) 24 μg cm^{-2}, (b) 48 μg cm^{-2}, (c) 120 μg cm^{-2}, (d) 240 μg cm^{-2}, and (e) 480 μg cm^{-2}. The scan rate of (B) and (C) was 10 mV s^{-1}. All solutions were saturated with N_2.

However, at a carbon nanotube (CNT) electrode, Stevenson's group[22] and Gorski's group[23] observed no changes for the redox peaks of GOx when the CNT–GOx electrodes were placed in the O_2-free testing solution with glucose, and concluded no DET between catalytic center of GOx and the CNT electrode. It has been reported that functional nanomaterials could provide an electron-mediating function to facilitate the DET of enzymes by reducing the electron tunnelling distance between their active sites and the electrode; therefore, there are already several papers reporting the detection of glucose based on the DET of glucose oxidase, such as by electrochemically entrapping GOx in the inner wall of the highly ordered conductive polyaniline nanotubes;[24] covalently cross-linking GOx to a boron-doped diamond electrode;[25] and incorporating GOx into the reduced graphene oxide-multiwalled carbon nanotube dispersion.[26] The results of these published investigations confirmed the bioelectrocatalytic activity of the electrical contacted GOx to the above-mentioned nanomaterials in the N_2-saturated testing solutions with the addition of glucose. In our design, AuNPs were attached to the surface of GOx near the flavin adenine dinucleotide (FAD) centre. This point of attachment facilitated the DET of the enzymes, probably by decreasing the electron-transfer distance between the catalytic centre and the electrode.[27]

The current density of the bioanode, i, also depends on the concentration of GOx (Γ_{GOx}) covering the bioanode. Γ_{GOx} was mainly affected by the amount of the graphene–AuNP hybrid covering the Au substrate, which controlled the binding of GOx. In order to estimate the optimal Γ_{GOx}, a series of bioanodes with various amounts of the graphene–AuNP–GOx were fabricated. Fig. 1C shows the relationship between the reduction currents of the bound GOx and the amount of the graphene–AuNP hybrid. With an increase of the loading amount of the graphene–AuNP hybrid from 24 μg cm^{-2} to 240 μg cm^{-2}, the reduction currents produced by the bound GOx increased linearly. The reduction current reached a maximum value of 155 μA cm^{-2}, and remained almost unchanged when the amount of the graphene–AuNP hybrid covered on the Au substrate was increased to more than 240 μg cm^{-2}. Also, different concentrations of GOx for the fabrication of the bioanode were tested (Fig. S4 in the ESI†), and 10 mg mL^{-1} was demonstrated to be the optimal concentration.

3.2 The characteristics of the biocathode

For the reason mentioned above, Au substrate was also chosen as the biocathode material. In the biocathode compartment, the oxygen was reduced to water at the biocathode as follows:

$$O_2 + 4H^+ + 4e \xrightarrow{\text{laccase}} 2H_2O \quad E_c^{o'} = 0.93\ \text{V}\ (vs.\ \text{SHE}) \qquad (3)$$

where $E_c^{o'}$ is the formal potential at pH 5.0, which was calculated by using the Nernst equation in the electrolyte solution saturated with O_2 according to the standard potential of the O_2/H_2O couple (1.23 V *vs.* SHE).[17] The OCP of the biocathode (E_c^{ocp}) was calculated to be 0.69 V. The measurement of the OCP for biocathode (E_c^{ocp}) was similar to that of E_a^{ocp}, where only the glucose in the electrolyte was replaced with saturated O_2. ABTS was the suitable electron mediator to decrease the over-potential for the reduction of O_2 by laccase in the cathode.[28] Once 0.5 mM ABTS was added into the catholyte, the E_c^{ocp} gradually approached 0.56 ± 0.02 V ($n = 3$) (see curves a and b of Fig. 2A).

In the acidic buffer solution, CV testing showed that the $ABTS^{2-}$ could be partly converted to $HABTS^-$ (Fig. S5 in the ESI†). The $ABTS^{\bullet-}/HABTS^-$ redox couple is better than $ABTS^{\bullet-}/ABTS^{2-}$ for the reduction of O_2 by laccase because the standard potentials of $ABTS^{\bullet-}/HABTS^-$ and $ABTS^{\bullet-}/ABTS^{2-}$ are 0.57 V and 0.44 V *vs.* SCE, respectively.[29] Interestingly, it was observed that the redox potential of the $ABTS^{\bullet-}/HABTS^-$ couple was around 0.55 V (*vs.* SCE) at the graphene–AuNP hybrid electrode (Fig. S5 in the ESI†), which is consistent with the measured E_c^{ocp}. This result is due to the adsorption of the acidic media being superior at the surfaces of the AuNPs,[16] and more $HABTS^-$ (which is more effective for the reduction of O_2) should thus form at the surface of the electrode. The UV-Vis spectrum (Fig. S6 in the ESI†) also demonstrated that $HABTS^-$ was appropriate as the electron mediator for the reduction of O_2 by laccase. The optimal concentration of the ABTS was selected to be 0.5 mM, as discussed in Fig. S7 in the ESI,† and the performance of ABTS for the reduction of O_2 at the biocathode is shown in Fig. 2B.

3.3 The characteristics of the EBFC

The EBFC was constructed from the bioanode and biocathode as described. The power density of the EBFC was influenced by the glucose concentration.[30,31] The results obtained in the EBFC revealed that the greatest E_{cell}^{ocv} and P_{max} were obtained when the glucose concentration was 50 mM (Fig. S8 in ESI†). The theoretical value of E_{cell}^{ocv} was calculated to be 1.28 V for the designed EBFC model. The measurement for E_{cell}^{ocv} is shown in Fig. 3A. As expected, the E_{cell}^{ocv} reached 1.16 ± 0.02 V ($n = 3$, curve a in Fig. 3A). The E_{cell}^{ocv} was considerably improved relative to those in the reports listed in Table 1.

Fig. 3B shows the polarization curve and the power density curve of the EBFC. During operation of the EBFC, the output voltage (E_{cell}) in the EBFC could be expressed in terms of the overpotentials associated with different fundamental phenomena as shown the equation: $E_{cell} = E_c^{ocp} - iR_{act,c} -$

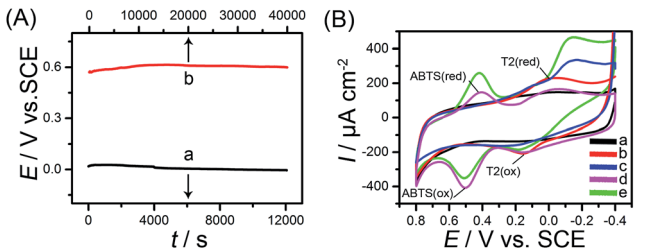

Fig. 2 (A) OCP of the graphene–AuNP–laccase hybrid electrode in pH 5.0 electrolyte solution saturated with O_2, (a) without ABTS and (b) containing 0.5 mM ABTS. (B) CVs of the graphene–AuNP electrode (a), graphene–AuNP–laccase hybrid electrode in pH 5.0 electrolyte solution saturated with N_2 (b) and saturated with O_2 (c), the graphene–AuNP–laccase hybrid electrode in pH 5.0 electrolyte solution containing 0.5 mM ABTS saturated with N_2 (d) and saturated with O_2 (e). The scan rate was 10 mV s^{-1}.

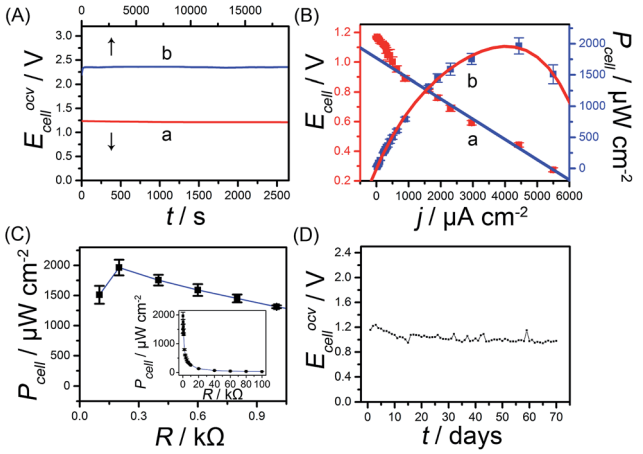

Fig. 3 (A) The E_{cell}^{ocv} of (a) a single EBFC unit and (b) two EBFCs units in series. (B) (a) Polarization curve and (b) power density curve of the EBFC, with every point being an average value of three independent measurements. (C) Power density of the EBFC *versus* the variable external loads. Inset: the power density *versus* the variable external loads from 100 Ω to 100 kΩ. (D) The relationship between E_{cell}^{ocv} of the EBFC and operation time.

Table 1 Comparison of our EBFC with other EBFCs

P_{max} (μW cm^{-2})	E_{cell}^{ocv} (V)	C (mM)	Electrode material	Ref. no.
1964 ± 130	1.16	50	Graphene–AuNP hybrid	Present
24.3 ± 4	0.58	100	Graphene	18
1450 ± 240	0.80	400	Carbon fiber sheet	12
740	0.83	15	Carbon nanotube fibers	19
350	0.88	15	Carbon fibers	33
1.36	0.884	1000	Graphite plates	34
1300	0.95	50	Carbon nanotube	10

$iR_{conc,c} - E_a^{ocp} - iR_{act,a} - iR_{conc,a} - ir_{ohm}$, where the symbols were defined previously.[32] E_{cell} was affected by the overpotentials derived from charge transfer, the concentration overpotentials, and the ohmic overpotentials of the EBFC. Because the EBFC performed generally in the region of the ohmic polarization, the overpotentials derived from charge transfer and the concentration overpotentials could be ignored, and E_{cell} could be expressed as $E_{cell} = E_c^{ocp} - E_a^{ocp} - ir_{ohm} = E_{cell}^{ocv} - ir_{ohm}$, which showed a linear relationship between E_{cell} and i in the region of the ohmic polarization. Based on the linear portion of the polarization curve in Fig. 3B ($E_{cell} = -266i + 1.03$, $R = 0.997$), the internal resistance of the EBFC (r_{ohm}) was calculated to be about 266 Ω. The power density as a function of the cell current density for the EBFC presented the typical bell-shaped curve[10] as shown in Fig. 3B, curve b. Thus, the maximum power output for the EBFC model, P_{max}, was estimated to be as high as 1.96 ± 0.13 mW cm^{-2} (relative to the geometric area of the Au substrate electrode). Under the optimal conditions, the maximal power output of the biofuel cell in the absence of glucose was only 0.231 ± 0.009 mW cm^{-2} and that in the absence of O_2 was only 0.281 ± 0.008 mW cm^{-2}; the maximal power output of the biofuel cell in the absence of glucose oxidase in the bioanode was only 0.447 ± 0.018 mW cm^{-2} and that in the absence of laccase in the biocathode was 0.512 ± 0.011 mW cm^{-2}, which demonstrated that the response was due only to glucose oxidation catalyzed by glucose oxidase and oxygen reduction catalyzed by laccase (in Fig. S9 in the ESI).† When the EBFC reached the maximum power output, the external load was equal to the r_{ohm}, about 200 Ω, as shown in Fig. 3C. Compared to the P_{max} values of other EBFCs reported in Table 1, the P_{max} achieved in this work was the highest.

A reasonable lifetime for portable applications[3] and a low capacity loss under open-circuit conditions[35] are of great importance for energy production and storage devices. EBFCs suffer from a very prominent disadvantage for long-term operation due to the loss in enzyme activity.[18,34] To test the storage stability of the EBFC, the E_{cell}^{ocv} was continuously measured over 70 days in a quiescent state. Fig. 3D showed that the E_{cell}^{ocv} could reach 94% of the maximal E_{cell}^{ocv} immediately once the EBFC was assembled. When the E_{cell}^{ocv} was lower than 1 V, the fuels in EBFC were replaced. After 70 days, the E_{cell}^{ocv} of the EBFC still retained 80% of its maximum value. For evaluating the stability of power output for the EBFC, the P_{max} of the EBFC was also tested every day (Fig. S10†). After operating for about 70 days, the P_{max} of the EBFC decreased to around 1.30 mW cm^{-2}, which was about 66% of its optimal value. GOx activity was reported to deteriorate in an acetic acid buffer solution (pH 5.0) after 4 days,[34] and the P_{max} of the reported EBFC was found to be 50% of its original value after 7 days for a graphene electrode.[18] However, the stability of the currently designed EBFC was improved greatly. This improvement may have been due to AuNPs providing a suitable microenvironment for the enzymes to retain their biological activities. Therefore, the graphene–AuNP hybrid was a suitable material for the preparation of the EBFC.

The potential value of the EBFC as a power source was also studied. E_{cell}^{ocv} of the two as-prepared EBFCs in series could reach about 2.36 V (Fig. 3A, curve b), which is the sum of the E_{cell}^{ocv} contributed by two EBFCs, respectively; the designed EBFCs in series could light red and yellow light-emitting diodes (LEDs) brightly (Fig. S11 in the ESI†).

4. Conclusions

In summary, based on a graphene–AuNP–GOx bioanode and graphene–AuNP–laccase biocathode, a novel EBFC was successfully fabricated. Because of fast electron transfer from the bioanode and biocathode, the constructed EBFC has high E_{cell}^{ocv} and power output. Both the as-prepared EBFC units in series can light up red and yellow LEDs, and the E_{cell}^{ocv} and P_{max} of the EBFC retain 80% and 66% of their maximum values after 70 days, respectively. We expect that the proposed strategy will advance the fabrication of EBFCs for practical applications.

Acknowledgements

We gratefully appreciate the National Natural Science Foundation (21175065, 21375059, 21335004 and 21121091), and the National Basic Research Program (2011CB933502) of China.

Notes and references

1 M. J. Moehlenbrock and S. D. Minteer, *Chem. Soc. Rev.*, 2008, **37**, 1188.
2 M. J. Cooney, V. Svoboda, C. Lau, G. Martin and S. D. Minteer, *Energy Environ. Sci.*, 2008, **1**, 320.
3 S. C. Barton, J. Gallaway and P. Atanassov, *Chem. Rev.*, 2004, **104**, 4867.
4 X. Y. Yang, G. Tian, N. Jiang and B. L. Su, *Energy Environ. Sci.*, 2012, **5**, 5540.
5 A. Heller, *Phys. Chem. Chem. Phys.*, 2004, **6**, 209.
6 U. Schroder, *Angew. Chem., Int. Ed.*, 2012, **51**, 7370.
7 A. Szczupak, J. Halamek, L. Halamkova, V. Bocharova, L. Alfonta and E. Katz, *Energy Environ. Sci.*, 2012, **5**, 8891.
8 T. Miyake, K. Haneda, N. Nagai, Y. Yatagawa, H. Onami, S. Yoshino, T. Abe and M. Nishizawa, *Energy Environ. Sci.*, 2011, **4**, 5008.
9 I. Willner, *Science*, 2002, **298**, 2407.
10 A. Zebda, C. Gondran, A. Le Goff, M. Holzinger, P. Cinquin and S. Cosnier, *Nat. Commun.*, 2011, **2**, 370.
11 S. Freguia, B. Virdis, F. Harnisch and J. Keller, *Electrochim. Acta*, 2012, **82**, 165.
12 H. Sakai, T. Nakagawa, Y. Tokita, T. Hatazawa, T. Ikeda, S. Tsujimura and K. Kano, *Energy Environ. Sci.*, 2009, **2**, 133.
13 Y. Chen, Y. Li, D. Sun, D. B. Tian, J. R. Zhang and J. J. Zhu, *J. Mater. Chem.*, 2011, **21**, 7604.
14 N. Mano, F. Mao, W. Shin, T. Chen and A. Heller, *Chem. Commun.*, 2003, **4**, 518.
15 X. H. Li, L. Dai, Y. Liu, X. J. Chen, W. Yan, L. P. Jiang and J. J. Zhu, *Adv. Funct. Mater.*, 2009, **19**, 3120.
16 Y. Onal, S. Schimpf and P. Claus, *J. Catal.*, 2004, **223**, 122.
17 D. C. Harris, *Quantitative chemical analysis*, W. H. Freeman and Company, New York, 8th edn, 2010.
18 C. Liu, S. Alwarappan, Z. F. Chen, X. X. Kong and C. Z. Li, *Biosens. Bioelectron.*, 2010, **25**, 1829.
19 F. Gao, L. Viry, M. Maugey, P. Poulin and N. Mano, *Nat. Commun.*, 2010, **1**, 2.
20 J. R. Bard and L. R. Faulkner, *Electrochemical Methods: Fundamentals and Applications*, Wiley, New York, 2nd edn, 2001.
21 C. S. Shan, H. F. Yang, J. F. Song, D. X. Han, A. Ivaska and L. Niu, *Anal. Chem.*, 2009, **81**, 2378.
22 J. M. Goran, S. M. Mantilla and K. J. Stevenson, *Anal. Chem.*, 2013, **85**, 1571.
23 M. Wooten, S. Karra, M. Zhang and W. Gorski, *Anal. Chem.*, 2014, **86**, 752.
24 Z. Y. Wang, S. N. Liu, P. Wu and C. X. Cai, *Anal. Chem.*, 2009, **81**, 1638.
25 Y. F. Bai, T. B. Xu, J. H. Luong and H. F. Cui, *Anal. Chem.*, 2014, **86**, 4910.
26 W. Grosse, J. Champavert, S. Gambhir, G. G. Wallace and S. E. Moulton, *Carbon*, 2013, **61**, 467.
27 J. T. Holland, C. Lau, S. Brozik, P. Atanassov and S. Banta, *J. Am. Chem. Soc.*, 2011, **133**, 19262.
28 Y. Liu, M. K. Wang, F. Zhao, B. F. Liu and S. J. Dong, *Chem.–Eur. J.*, 2005, **11**, 4970.
29 S. L. Scott, W. J. Chen, A. Bakac and J. H. Espenson, *J. Phys. Chem.*, 1993, **97**, 6710.
30 N. Mano, *Chem. Commun.*, 2008, **19**, 2221.
31 D. Wen, X. L. Xu and S. J. Dong, *Energy Environ. Sci.*, 2011, **4**, 1358.
32 F. Zhao, R. C. T. Slade and J. R. Varcoe, *Chem. Soc. Rev.*, 2009, **38**, 1926.
33 V. Soukharev, N. Mano and A. Heller, *J. Am. Chem. Soc.*, 2004, **126**, 8368.
34 S. Fishilevich, L. Amir, Y. Fridman, A. Aharoni and L. Alfonta, *J. Am. Chem. Soc.*, 2009, **131**, 12052.
35 S. K. Chaudhuri and D. R. Lovley, *Nat. Biotechnol.*, 2003, **21**, 1229.